

Electron structure and optical properties of technetium

V. N. Antonov, M. M. Kirillova, E. E. Krasovskii, and Yu. S. Ponosov

Institute of Metal Physics, Ural Division of the Academy of Sciences of the USSR, Sverdlovsk

(Submitted 18 December 1987)

Zh. Eksp. Teor. Fiz. **94**, 192–198 (September 1988)

The self-consistent linear method of augmented plane waves is used to calculate the energy band structure and the density of states $N(E)$ of hexagonal technetium. A matrix element of the dipole transitions is used to calculate the frequency dependence of the interband optical conductivity $\sigma(\omega)$ and of the real part $\varepsilon_1(\omega)$ of the complex permittivity for two directions of polarization of an optical wave relative to the hexagonal c axis of the crystal ($\mathbf{E} \perp c$ and $\mathbf{E} \parallel c$). The anisotropy of the optical absorption is considered in the photon energy range $\hbar\omega = 0-25$ eV. An experimental investigation is reported of the optical properties of a Tc film with the (0001) orientation at photon energies $E = 0.62-10$ eV. A strong absorption band is attributed to the ($d-d, p$) electron transitions. It is shown that there is a satisfactory agreement between the experimentally observed and calculated functions $\sigma_{\perp}(\omega)$ and $\varepsilon_{\perp}^1(\omega)$.

Technetium is a transition metal with a partly filled $4d$ shell and it crystallizes in the hcp lattice. Among the d metals, Tc is distinguished by a relatively high temperature of the transition to the superconducting state ($T_c = 7.82$ K is reported in Ref. 1) and this is the reason for the special interest in the electron and phonon spectra of this element.

Theoretical calculations of the electron structure and some physical properties of technetium have been carried out for fcc crystals²⁻⁵ as well as for the hcp structure.⁶⁻⁸ For example, the method of augmented plane waves (APW) is used in Ref. 3 to obtain estimates of Tc. The authors of Ref. 7 use a linear augmented plane wave (LAPW) method to calculate the dispersion of the energy bands, the density of states, and the intensities of the L_{III} , M_V , and N_{III} x-ray emission spectra. The APW method is used in Ref. 8 to find the dispersion of the imaginary part $\varepsilon_2(\omega)$ of the permittivity (ω is the angular frequency of an optical wave) in the approximation of a constant matrix element of the transition. The most detailed calculations of the energy band spectrum and of the complex permittivity $\varepsilon(\omega)$ of technetium (for fcc and bcc phases) are reported in Ref. 4: they were carried out allowing for the energy dependence of the matrix element of a transition and using the linear muffin-tin orbital (LMTO) method. These results were also used to analyze the spectrum of characteristic electron energy losses. However, the experimental data on the spectral characteristics of technetium, which might confirm the validity of the calculations of its energy band structure, are still lacking.

We shall describe the first study of some of the optical properties of Tc and a theoretical calculation of the complex permittivity $\varepsilon(\omega)$ carried out allowing for a matrix element of a transition in the hcp lattice. We shall analyze the characteristics of the interband optical absorption and their relationship to the structure of the energy bands, and also to the anisotropy of the optical properties.

1. EXPERIMENTAL DATA

Our optical investigations were carried out on a film sample of Tc prepared by ionic sputtering with magnetic focusing of the beam when the pressure of the working gas (Kr) in the chamber was 10^{-3} Pa (Ref. 9). The temperature of a polished glass substrate was close to that of liquid nitro-

gen and the deposition rate was 1 nm/min. The starting material was the ⁹⁹Tc isotope. The film thickness was 120 nm. The results of an x-ray structure analysis showed that the films of this kind had the hcp structure and were textured in such a way that the (0001) basal plane formed the surface with a misorientation angle of $\lesssim 10^\circ$. The resistivity ratio of the investigated film was $\rho_{295\text{ K}}/\rho_{4.2\text{ K}} = 3.5$. The temperature of the transition to the superconducting state was $T_c = 8.2$ K.

The refractive index n and the extinction coefficient k of technetium were determined in the wavelength range 0.25–2.0 μm inside the vacuum chamber employing the polarimetric Beattie method accurate to within 2–3%. A hexagonal crystal had two components of the permittivity tensor: $\varepsilon_{\parallel} = (n_{\parallel} - ik_{\parallel})^2$ and $\varepsilon_{\perp} = (n_{\perp} - ik_{\perp})^2$, which characterized the propagation of optical waves along ($\mathbf{E} \parallel c$) and at right-angles ($\mathbf{E} \perp c$) to the c crystal axis (here, \mathbf{E} is the electric vector of a plane-polarized wave). The optical constants measured in the basal plane represented n_{\perp} and k_{\perp} with an error to within terms $1/|\varepsilon|$ compared with unity. In the case of our textured samples the corrections to n_{\perp} and k_{\perp} associated with some misorientation of the (0001) planes relative to the direction of polarization \mathbf{E} did not exceed the experimental error ($\sim 3\%$). The numerical values of the optical constants of technetium were determined in this way (Table I). They were then used to calculate the optical conductivity $\sigma_{\perp} = n_{\perp} k_{\perp} \omega / 2\pi$ and the real part $\varepsilon_{\perp}^1 = n_{\perp}^2 - k_{\perp}^2$ of the permittivity. In the wavelength range $\lambda = 0.12-0.25$ μm we used the same sample to determine the reflectivity R in unpolarized light. The optical constants were found in this short-wavelength part of the spectrum using the Kramers-Kronig relationships. The calculation method was described in Ref. 10.

2. METHOD OF CALCULATION OF THE ENERGY BAND STRUCTURE

The band structure of Tc was calculated in a self-consistent manner at 222 points of the irreducible part of the Brillouin zone. The crystal potential was determined in accordance with the scheme of Ref. 11 allowing for the exchange and correlation on the basis of the methods of Hedin and Lundqvist.¹² The resultant wave functions of the electron

TABLE I. Optical constants of technetium.

λ, μ	n_{\perp}	k_{\perp}	λ, μ	n_{\perp}	k_{\perp}	λ, μ	n_{\perp}	k_{\perp}
0.250	1.15	3.00	0.520	3.30	4.14	0.825	3.56	4.75
0.260	1.22	3.12	0.530	3.32	4.17	0.850	3.54	4.85
0.270	1.30	3.23	0.540	3.34	4.18	0.875	3.53	4.93
0.280	1.39	3.32	0.550	3.36	4.21	0.900	3.50	5.02
0.290	1.47	3.42	0.560	3.39	4.23	0.925	3.50	5.10
0.300	1.62	3.59	0.570	3.42	4.25	0.950	3.51	5.20
0.310	1.70	3.62	0.580	3.44	4.26	0.975	3.48	5.29
0.320	1.77	3.78	0.590	3.46	4.28	1.00	3.46	5.25
0.330	1.83	3.95	0.600	3.47	4.29	1.05	3.43	5.50
0.340	1.95	4.04	0.610	3.49	4.30	1.10	3.38	5.51
0.350	2.07	4.13	0.625	3.48	4.37	1.15	3.25	5.47
0.360	2.21	4.21	0.630	3.47	4.46	1.20	3.15	5.60
0.370	2.36	4.30	0.640	3.49	4.48	1.30	3.05	5.92
0.380	2.51	4.30	0.650	3.51	4.49	1.35	2.97	6.05
0.390	2.61	4.24	0.660	3.54	4.50	1.40	3.20	6.26
0.400	2.73	4.20	0.670	3.56	4.50	1.45	3.36	6.47
0.410	2.86	4.13	0.680	3.57	4.51	1.50	3.35	6.65
0.420	2.90	4.15	0.690	3.59	4.52	1.55	3.36	6.86
0.430	2.96	4.14	0.700	3.59	4.52	1.60	3.45	7.16
0.440	3.03	4.12	0.710	3.60	4.54	1.65	3.51	7.33
0.450	3.08	4.11	0.720	3.61	4.54	1.70	3.62	7.32
0.460	3.12	4.10	0.730	3.61	4.56	1.75	3.60	7.14
0.470	3.15	4.09	0.740	3.61	4.57	1.80	3.56	7.04
0.480	3.19	4.09	0.750	3.61	4.59	1.90	3.24	7.78
0.490	3.21	4.10	0.760	3.60	4.60	1.95	3.44	7.81
0.500	3.24	4.11	0.780	3.59	4.65	2.00	3.49	7.79
0.510	3.26	4.13	0.800	3.51	4.70	-	-	-

states were then used to find the matrix elements of the momentum operator for direct dipole transitions. This was done by a method developed in Ref. 13. The expansion of the wave functions included the fundamental vectors deduced from the reciprocal lattice vectors G_i , such that $|G_i| < G_0/a$ (a is the lattice constant), where $G_0 = 14.6$. Consequently, the size of the matrix of the Hamiltonian at the point Γ was 73×73 . This selection of G_0 ensured convergence of the squares of the moduli of the matrix elements to within an error not exceeding 5%. The optical conductivity was calculated from

$$\sigma(\omega) = \frac{2\pi e^2}{m^2 \omega} \sum_{i,i'} \int_{\text{BZ}} |\mathbf{e}_0 \mathbf{P}_{i,i'}(\mathbf{k})|^2 \delta(E_{i'}(\mathbf{k}) - E_i(\mathbf{k}) - \hbar\omega) \frac{d\mathbf{k}}{(2\pi)^3}. \tag{1}$$

Here, \mathbf{e}_0 is a unit vector along the direction of the electric field; $E_i(\mathbf{k})$ and $E_{i'}(\mathbf{k})$ are the band energies of the initial and final one-electron states, respectively; $\mathbf{P}_{i,i'}$ is the matrix element of the momentum operator between the initial and final states with the wave vector \mathbf{k} . In the calculation of the optical conductivity we allowed for the existence of 16 bands. Integration over the Brillouin zone (BZ) in Eq. (1) was carried out by the method of tetrahedra at 222 points, corresponding to the splitting of each 1/24th part of the Brillouin zone into 810 tetrahedra. The function $\epsilon_1(\omega)$ was calculated by the Kramers-Kronig method.

Figure 1 shows the dispersion curves $E(\mathbf{k})$ and the total density of states $N(E)$. An analysis of the partial densities of the s , p , d , and f states shows that the high values of $N(E)$ observed in the range 0.3–0.95 Ry are due to the d -type elec-

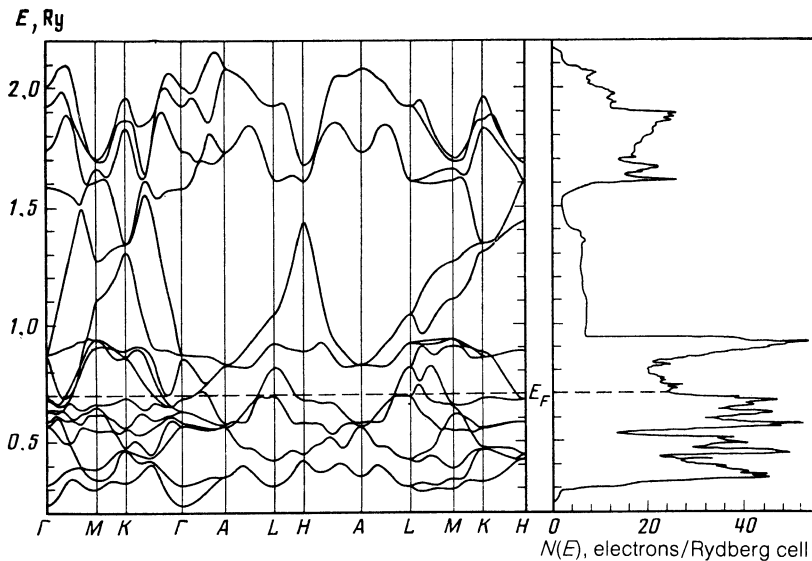


FIG. 1. Electron energy structure and the density of states $N(E)$ of hexagonal technetium.

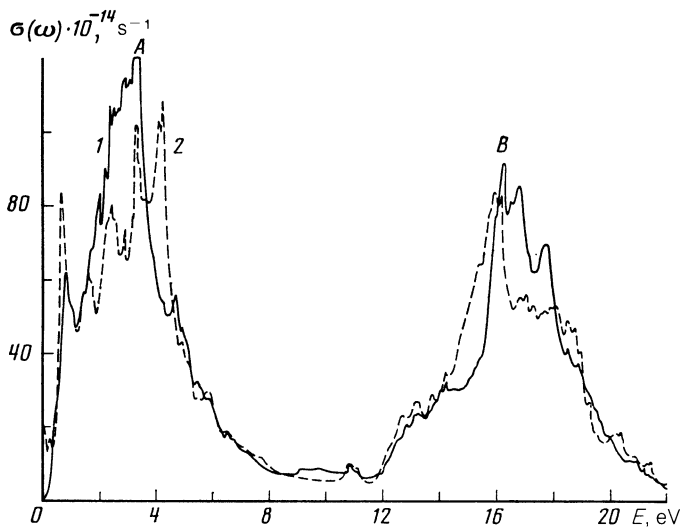


FIG. 2. Calculated interband optical conductivity $\sigma(\omega)$ of technetium: 1) σ_{\perp} ; 2) σ_{\parallel} .

trons. The second maximum of the $N(E)$ curve in the energy range 1.6–2.0 Ry is mainly due to free states with the p symmetry, although on the whole the p - f hybridization is considerable.

3. DISCUSSION OF RESULTS

Theoretical curves of the optical conductivity $\sigma(\omega)$ of technetium for the directions of polarization of the light wave $\mathbf{E} \parallel \mathbf{c}$ and $\mathbf{E} \perp \mathbf{c}$ are plotted in Fig. 2. Band calculations predict the existence of two strong interband absorption bands at photon energies $E = 0.2$ – 7.0 eV (A) and $E = 12$ – 22 eV (B). The first of these bands is due to electron transitions from the occupied part of the d energy band to free states which are also of the d -type. The high intensity of the first absorption band is due to strong hybridization of the d and p states in the filled part of the energy band (d - d , p transitions). The second absorption band is due to transitions from the occupied part of the d energy band to the free states of the p -type symmetry with an admixture of the f states (d - p , f transitions). It follows from the Fig. 2 that the energy positions of the main absorption bands A and B , governed by the width and relative positions of the dispersion curves $E(\mathbf{k})$, remain unchanged for the $\mathbf{E} \parallel \mathbf{c}$ and $\mathbf{E} \perp \mathbf{c}$ directions. However, the frequency dependences and the absolute val-

ues of the longitudinal σ_{\parallel} and transverse σ_{\perp} components of the optical conductivity are different, particularly in the range $E < 5$ eV.

The theory predicts also a strong anisotropy of the dispersion of $\varepsilon_{\parallel}^{\prime}$ and $\varepsilon_{\perp}^{\prime}$ (Fig. 3). In the interval between the strong (d - d , p) and (d - p , f) electron transitions ($E = 10.1$ – 10.3 eV) both functions $\varepsilon_{\parallel}^{\prime}$ and $\varepsilon_{\perp}^{\prime}$ pass through zero. Since in this range the imaginary part of the permittivity is low ($\varepsilon_2 \ll 1$), the conditions for a plasma resonance are satisfied. The second change of the sign of $\varepsilon_{\parallel}^{\prime}$ and $\varepsilon_{\perp}^{\prime}$ occurs at energies of 16.5 and 16.9 eV, respectively, and corresponds to a maximum of the high-energy absorption band B (Fig. 2). In this case the change in the sign of $\varepsilon_{\parallel}^{\prime}$ and $\varepsilon_{\perp}^{\prime}$ reflects only the anomalous dispersion of these functions in the region of strong interband transitions. The third zero in the frequency dependence at energies 21.3 eV ($\varepsilon_{\parallel}^{\prime}$) and 21.5 eV ($\varepsilon_{\perp}^{\prime}$), where $\varepsilon_2 \ll 1$ once again demonstrates the possibility of a plasma resonance.

An analysis of the function representing the characteristic losses $\text{Im}[-1/\varepsilon(\omega)]$ is outside the scope of the present paper. A detailed analysis of its spectral dependence had been made earlier^{4,5} for hypothetical technetium in the fcc lattice using the self-consistent LMTO method for the calculation of the energy band structure. We shall mention only

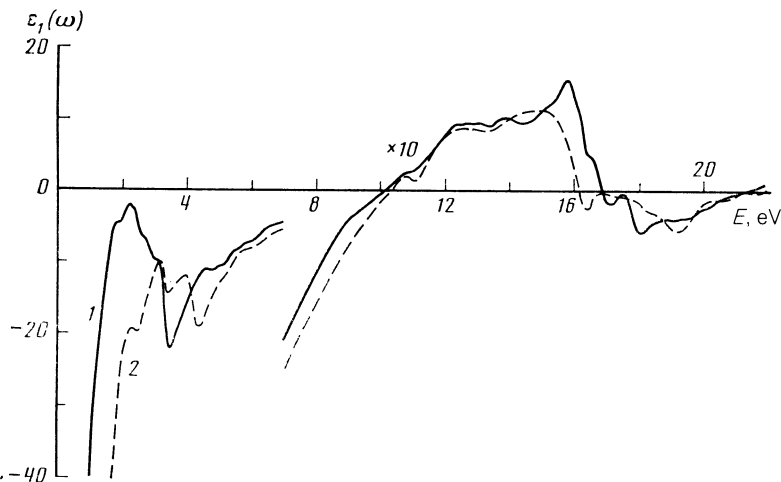


FIG. 3. Calculated real part $\varepsilon_1(\omega)$ of the complex permittivity of technetium: 1) $\varepsilon_{\perp}^{\prime}$; 2) $\varepsilon_{\parallel}^{\prime}$.

the validity of the hypothesis put forward in Refs. 4 and 5 that the nature of the crystal lattice has little influence on the optical properties of technetium. In fact, a comparison of the dependences $\sigma(\omega)$ and $\varepsilon_1(\omega)$ obtained in the present paper for the hcp phase with the corresponding curves for the fcc lattice of Tc (Refs. 4 and 5) shows that the agreement between the energy positions of the main optical conductivity bands and of the zeros of the real part of the permittivity is good, and significant differences are found only in the fine structure of the spectra.

An analysis of the partial contributions to σ_{\parallel} and σ_{\perp} makes it possible to identify the main pairs of the energy bands responsible for the absorption spectra. The absorption bands *A* and *B* of technetium (Fig. 2) are due to superposition of several contributions of electron transitions with similar energies. Some of them (for example, 8 → 11, 7 → 9, 6 → 8, 9) are induced by light of the same intensities of both crystallographic directions $\mathbf{E} \perp \mathbf{c}$ and $\mathbf{E} \parallel \mathbf{c}$, whereas others have different energy dependences of the intensity of the transition. For example, in the case of the $\mathbf{E} \parallel \mathbf{c}$ the partial contributions made to σ_{ij} by the 7 → 10, 11 transitions are weakened by a factor of two, whereas the 6 → 7, 10 and 5 → 8 transitions are enhanced by a factor of two compared with the $\mathbf{E} \perp \mathbf{c}$ case. In particular, the 6 → 10 transition between the flat part of the *d*

energy band in the vicinity of the *KH* and ΓK directions in the Brillouin zone forms a clear structure in σ_{\parallel} at 4 eV, which is missing from the transverse component σ_{\perp} (Fig. 2).

The σ_{\perp} and ε_1^{\perp} curves obtained by us experimentally and calculated theoretically using a matrix element are compared in Fig. 4. We can see that they are in satisfactory agreement. This is true of the energy positions of the principal features of the structure and of the absolute values of σ and ε_1 . The experimentally observed absorption peak of σ_{\perp} at 0.73 eV is in good agreement with the profile of the calculated narrow structure ($E = 0.75$ eV). The "inflections" in the experimental σ_{\perp} curve at energies 1.4, 1.7, 1.9, 2.2, and 4.4–5.0 eV correspond to sharp peaks of the calculated curve. The difference between the theoretical and experimental curves representing the optical conductivity consists not only in the smoother nature of the lattice, but also in higher values of $\sigma_{\perp}^{\text{theor}}$ in the region of the absorption band maximum. We can expect an allowance for the finite lifetime of the excited states of electrons to improve the agreement between the experimental and calculated results. We can nevertheless say that the experimentally observed optical absorption of technetium is explained satisfactorily and quantitatively by our calculations of the energy bands and the wave function of electrons.

The authors are grateful to M. B. Tsetlin for supplying Tc samples and for measuring their electrophysical properties, and to Yu. A. Dorofeev for x-ray structure analysis.

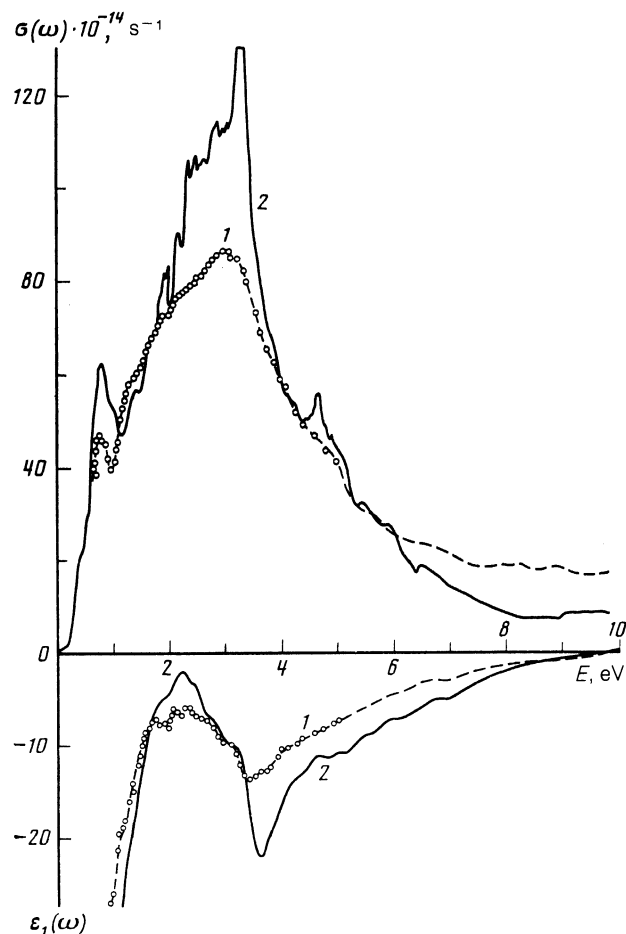


FIG. 4. Comparison of the experimental and calculated data for technetium: a) σ_{\perp} ; b) ε_1^{\perp} ; 1) experimental results; 2) calculated results. The dashed curve represents the experimental data deduced by the Kramers-Kronig method.

- ¹G. Kosterz, L. L. Isaacs, R. L. Panosh, and C. C. Koch, *Phys. Rev. Lett.* **27**, 304 (1971).
- ²V. L. Moruzzi, J. F. Janak, and A. R. Williams, *Calculated Electronic Properties of Metals*, Pergamon Press, Oxford (1978).
- ³D. A. Papacontantopoulos, L. L. Boyer, B. M. Klein, A. R. Williams, V. L. Moruzzi, and J. F. Janak, *Phys. Rev. B* **15**, 4221 (1977).
- ⁴I. I. Mazin, E. G. Maksimov, S. N. Rashkeev, and Yu. A. Uspenskiĭ, *Zh. Eksp. Teor. Fiz.* **90**, 1092 (1986) [*Sov. Phys. JETP* **63**, 637 (1986)].
- ⁵M. V. Zharnikov and S. N. Rashkeev, *Fiz. Tverd. Tela (Leningrad)* **26**, 3385 (1984) [*Sov. Phys. Solid State* **26**, 2034 (1984)].
- ⁶R. Asokamani, K. Iyakutti and V. Devanathan, *Solid State Commun.* **30**, 385 (1979).
- ⁷V. V. Nemoshkalenko, N. A. Plotnikov, and V. N. Antonov, *Metallofizika* **4**, No. 2, 18 (1982).
- ⁸P. Chatterjee, *Phys. Rev. B* **27**, 4722 (1983).
- ⁹V. M. Golyanov, L. A. Elesin, and M. N. Mikheeva, *Pis'ma Zh. Eksp. Teor. Fiz.* **18**, 569 (1973) [*JETP Lett.* **18**, 335 (1973)].
- ¹⁰E. S. Gluskin, A. V. Druzhinin, M. M. Kirillova, V. I. Kochubeĭ, L. V. Nomerovannaya, and V. M. Maevskiĭ, *Opt. Spektrosk.* **55**, 891 (1983) [*Opt. Spectrosc. (USSR)* **55**, 537 (1983)].
- ¹¹G. V. Vol'f, V. V. Dyakin, and V. P. Shirokovskiĭ, *Fiz. Met. Metalloved.* **38**, 949 (1974).
- ¹²L. Hedin and B. I. Lundqvist, *J. Phys. C* **4**, 2064 (1971).
- ¹³E. E. Krasovskiĭ, V. N. Antonov, and V. V. Nemoshkalenko, *Metallofizika* **8**, No. 5, 20 (1986).

Translated by A. Tybulewicz